

Introduction aux techniques non intrusives pour la caractérisation des écoulements à bulles

Prof. Maria Rosaria Vetrano



Introduction

- Very broad topic
- Different sizes, different shapes, embedded in transparent/opaque fluids.
- A large variety of applications and conditions (temperature, pressure,...)
- Techniques often developed cases-by-case

[Home](#) > [Experiments in Fluids](#) > Article

In situ measurements of void fractions and bubble size distributions in bubble curtains

Research Article | [Open access](#) | Published: 24 January 2023

Volume 64, article number 31, (2023) | [Cite this article](#)

Article | [Open access](#) | Published: 22 May 2018

Characterization of different bubble formulations for blood-brain barrier opening using a focused ultrasound system with acoustic feedback control

[Chenchen Bing](#) , [Yu Hong](#), [Christopher Hernandez](#), [Megan Rich](#), [Bingbing Cheng](#), [Imalka Munaweera](#), [Debra Szczepanski](#), [Yin Xi](#), [Mark Bolding](#), [Agata Exner](#) & [Rajiv Chopra](#)

Scientific Reports **8**, Article number: 7986 (2018) | [Cite this article](#)

4933 Accesses | 67 Citations | 5 Altmetric | [Metrics](#)

[Home](#) > [Journal of Hydrodynamics](#) > Article

Measurement and characterization of bulk nanobubbles by nanoparticle tracking analysis method

Articles | Published: 14 December 2022

Volume 34, pages 1121–1133, (2022) | [Cite this article](#)

Characterization of a chemical reaction in a bubble column using wire-mesh sensor and ultrafast X-ray CT

R. Kipping¹, E. Schleicher², H. Kryk², U. Hampel^{1,2}

¹AREVA Endowed Chair of Imaging Techniques in Energy and Process Engineering, Technische Universität Dresden, 01062 Dresden, Germany

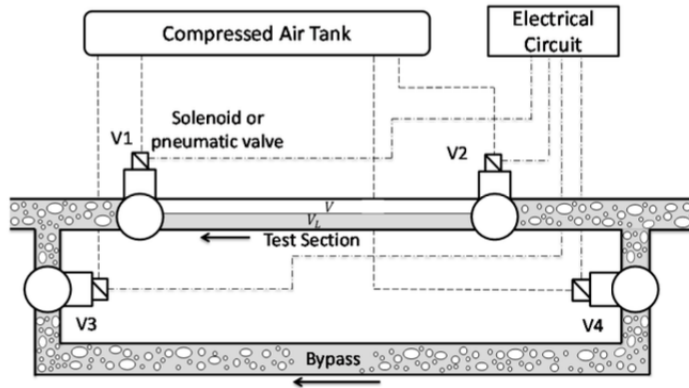
²Institute of Fluid Dynamics, Helmholtz-Zentrum Dresden-Rossendorf, Bautzner Landstr. 400, 01328 Dresden, Germany

*Corresponding author: ragna.kipping@tu-dresden.de

Void fraction

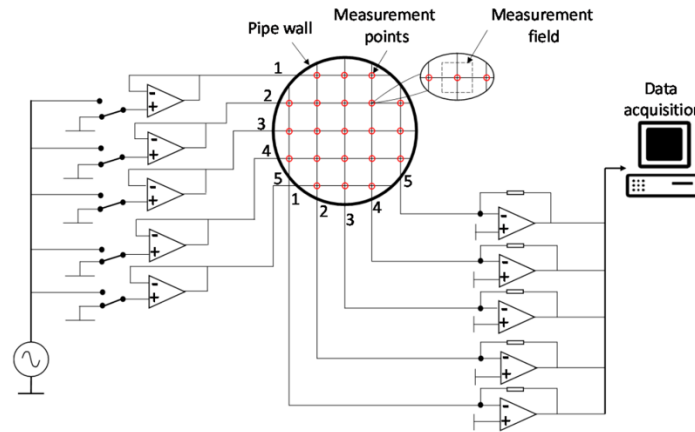
Sampling

Quick-Closing Valves

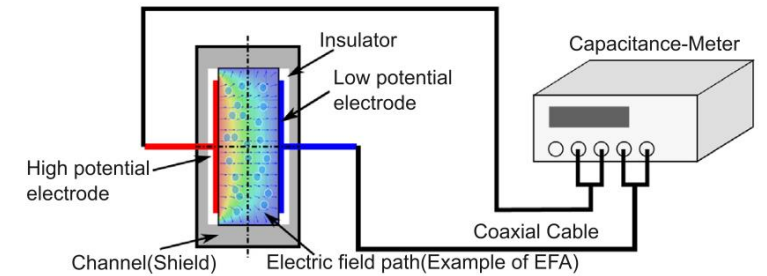


Intrusive

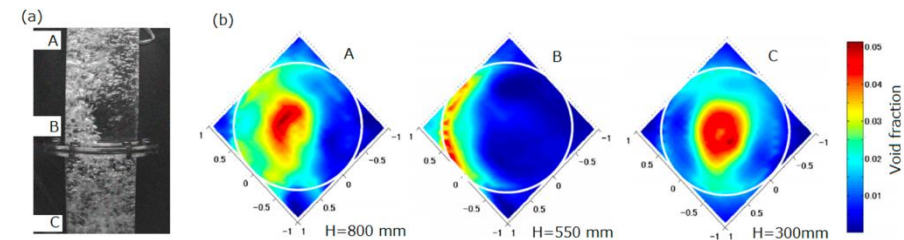
Wire-Mesh



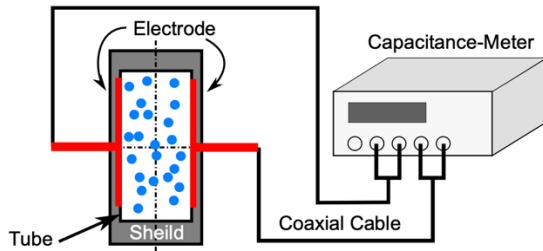
Capacity sensors



Ultrasonic sensors



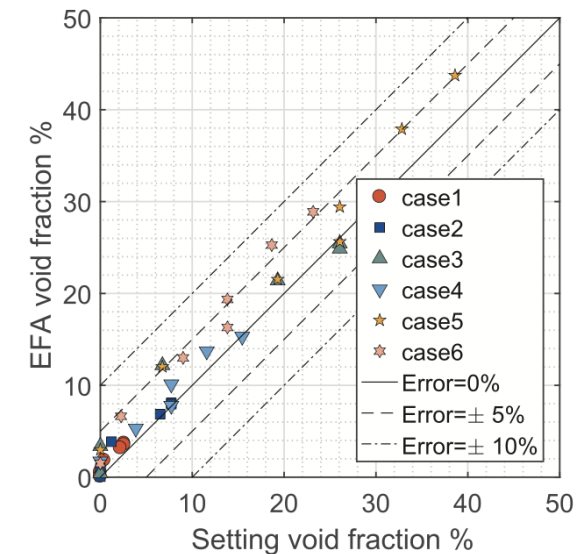
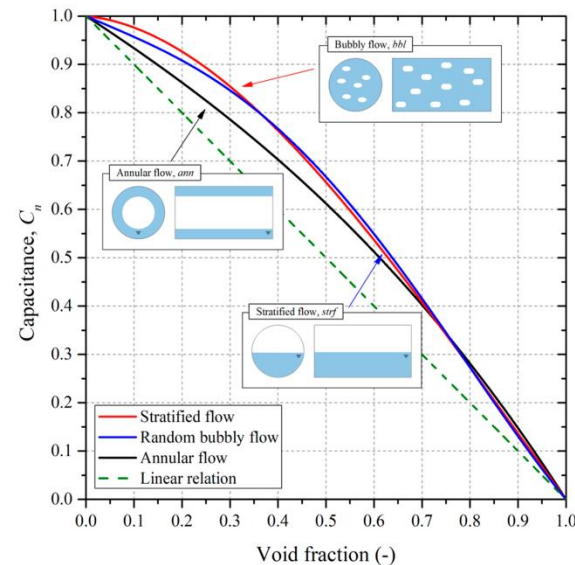
Capacitive sensor



$$\alpha = \frac{C_L - C_M}{C_L - C_G} \times 100[\%]$$

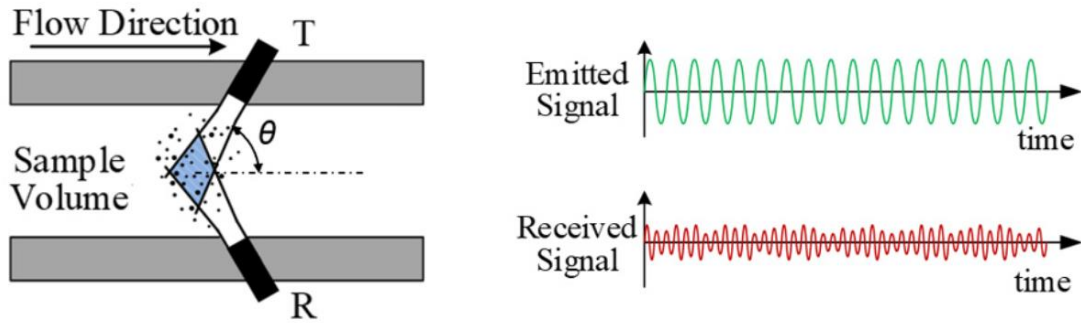
C_L is capacitance at the liquid phase,
 C_G is capacitance at the gaseous phase
 C_M is measured capacitance

- Principle**
- The void fraction is calculated by the measured capacitance, which changes due to the gas/liquid volume ratio.
 - The liquid dielectric constant is larger than the gas one, so the capacitance increases with liquid volume.
 - Finite element method-based simulations (Electric Field Analysis) to calibrate.
 - The design of the sensor should be optimized for the liquid and its temperature



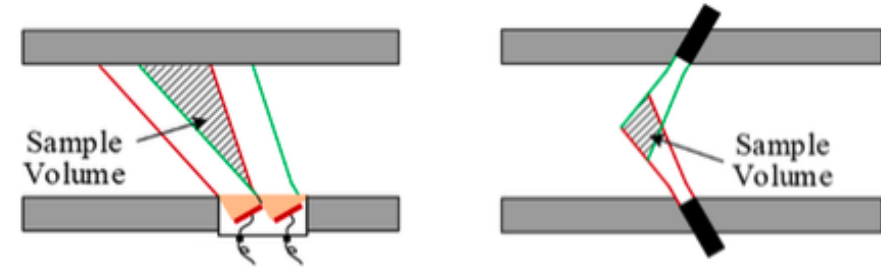
Ultrasonic sensor

Continuous-wave ultrasonic Doppler (CWUD)

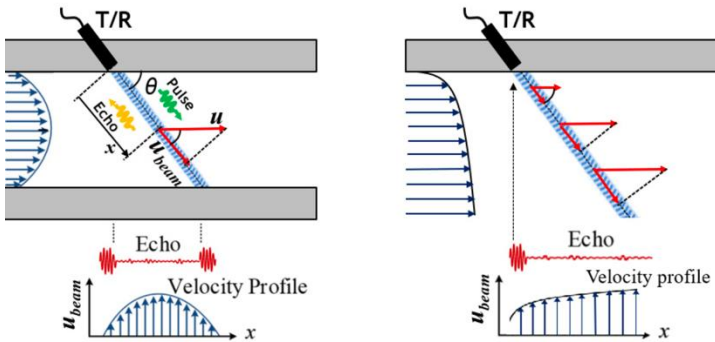


Principle velocity measurement

- Transducer T emits ultrasonic waves of frequency f_0 to the fluid
- Transducer R receives the waves with a frequency modulated according to the Doppler effect $f_d = \frac{2u \cos \theta}{c} f_0$
- When multiple bubbles are present in the sample volume, an average Doppler frequency $\langle f_d \rangle$ and an average velocity is calculated $\langle u_{Dop} \rangle$



Pulsed-wave ultrasonic Doppler (PWUD)



Principle velocity measurement

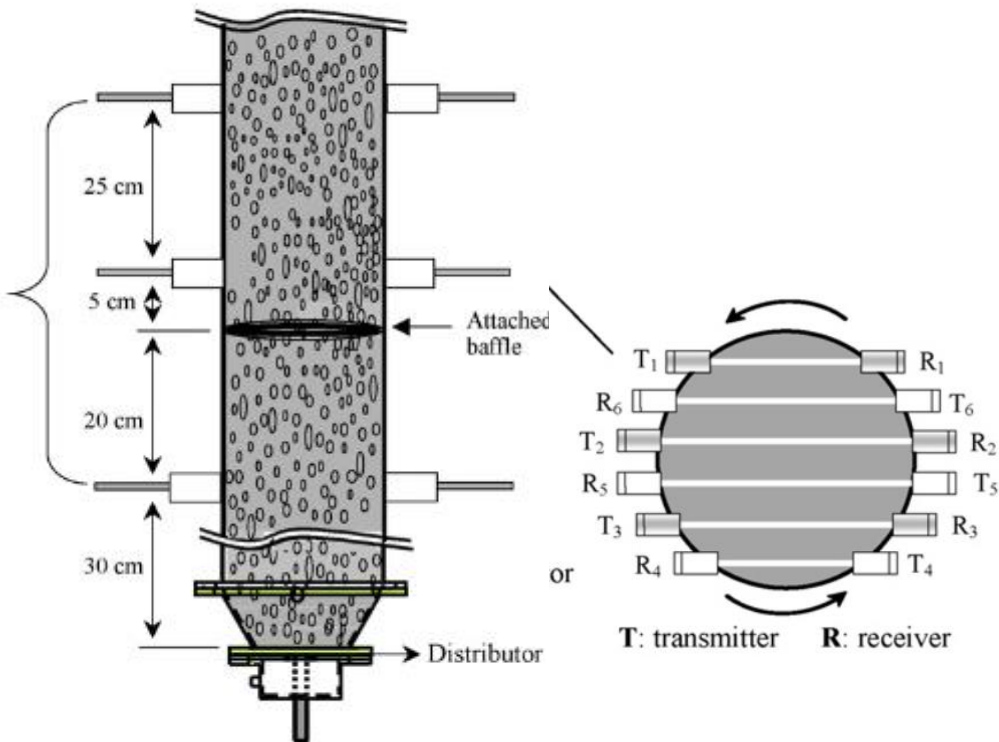
- One transducer emits and receives pulsed ultrasound waves.
- The measurement position x from which the pulse is reflected $x = \frac{c \Delta t}{2}$, varying Δt one varies the measurement volume position
- The phase shift obtained from the echo give de bubble velocity

Ultrasonic computed tomography

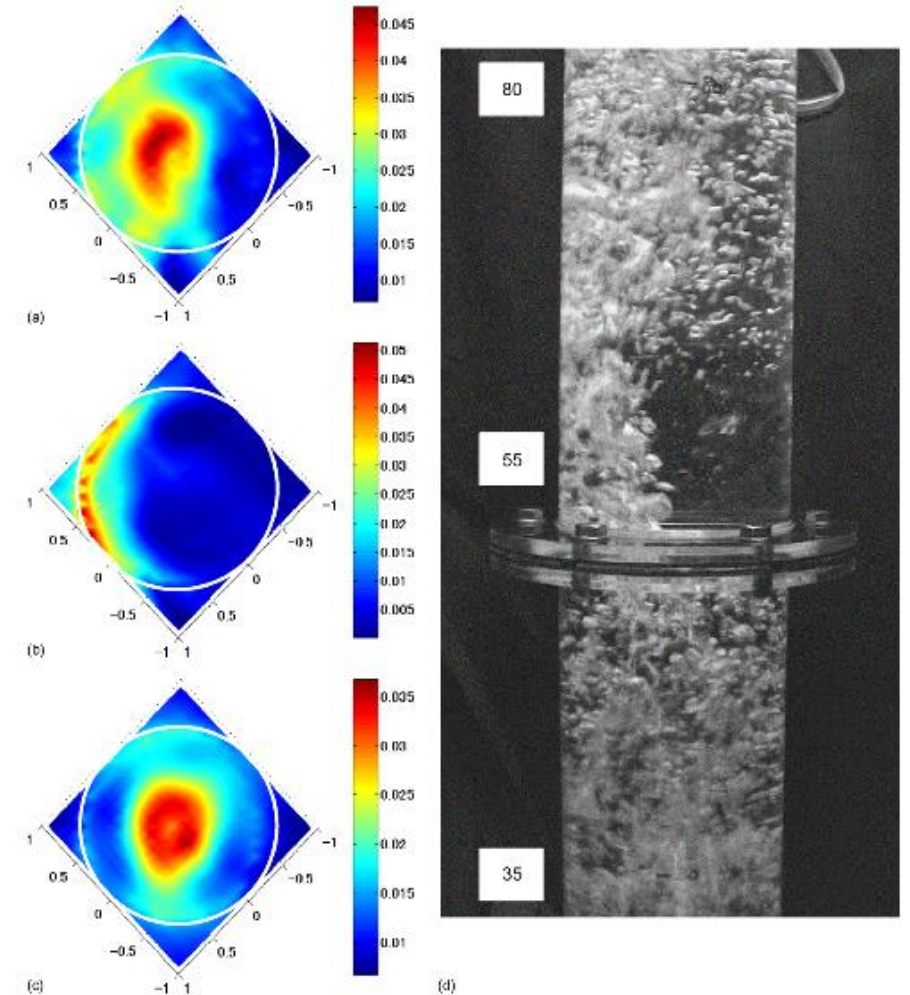
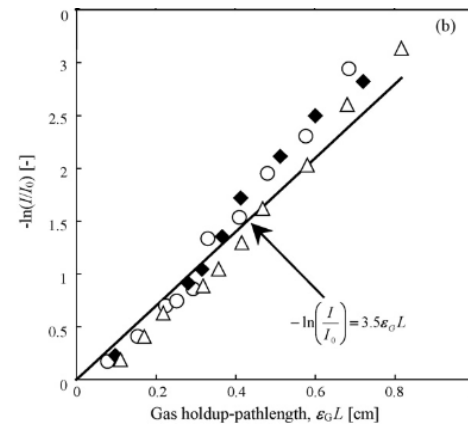
Example of void fraction field reconstruction

Principle void fraction (holdup) measurement

- Based on the attenuation of the sound waves
- Needs preliminary calibration
- Use Filtered Back Projection (FBP) to reconstruct 3D field



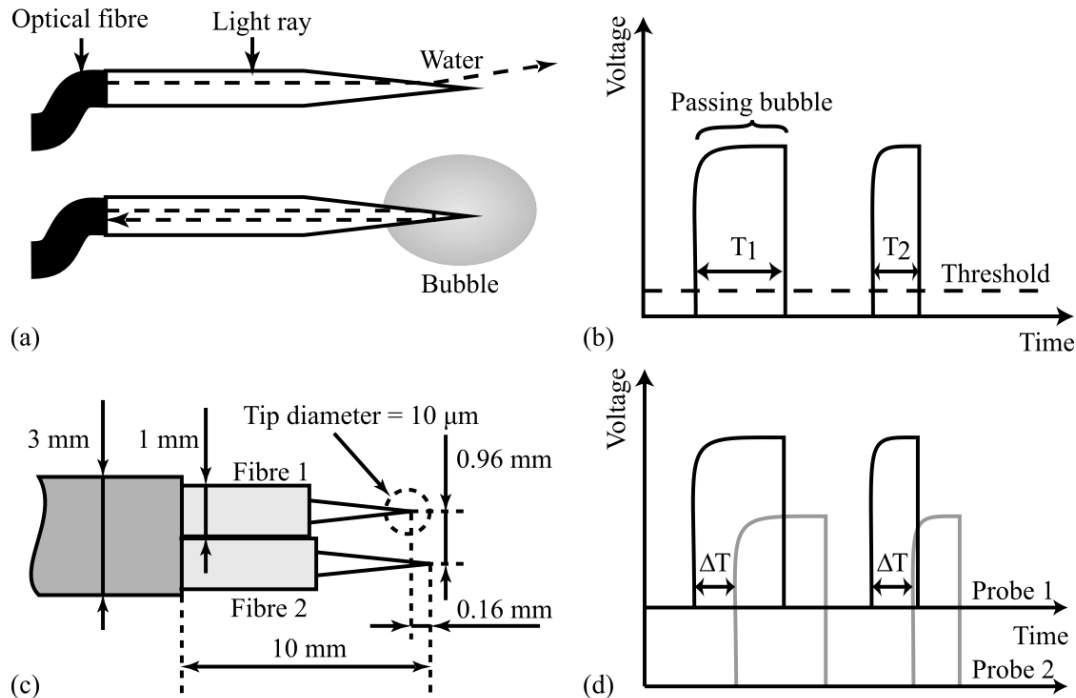
Preliminary calibration



Bubble size/velocity

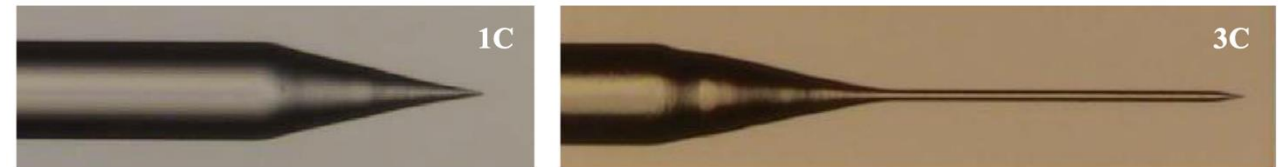
- Allows for accurate size, shape measurement, and velocity.
 - They require transparent media and can have limited resolution for very small bubbles.
 - They can fail if the void fraction is increased.
-
- **Phase Detection Probes**
 - **Backlighting/Shadowgraphy**
 - **Laser Diffraction Systems**
 - **Laser/Phase Doppler Anemometry**
 - **Glare points (GPVS)/ Glare Circles**
 - **ILIDS**
 - **CARS**

Phase Detection Probes



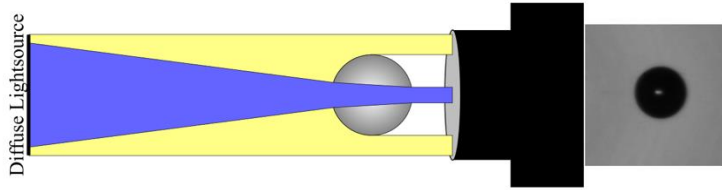
Principle

- When a bubble passes by, it causes the tip to pierce the surface, leading to total reflection of the light ray at the fiber-air interface due to the significant difference in refractive index.
- Using two tip configuration the velocity and size of the bubble can be determined.



Recent development of Optical-Fiber Doppler Probe (OFDP)

Backlighting

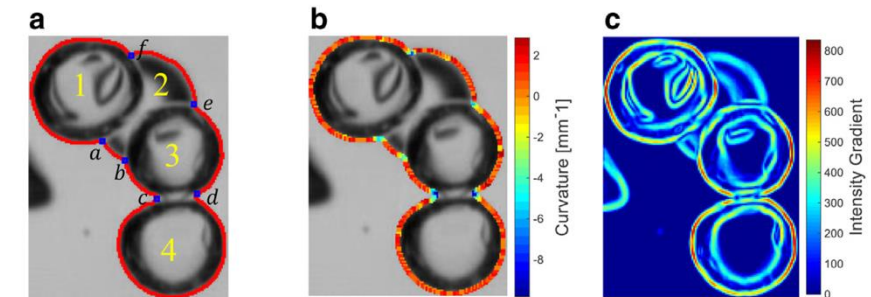
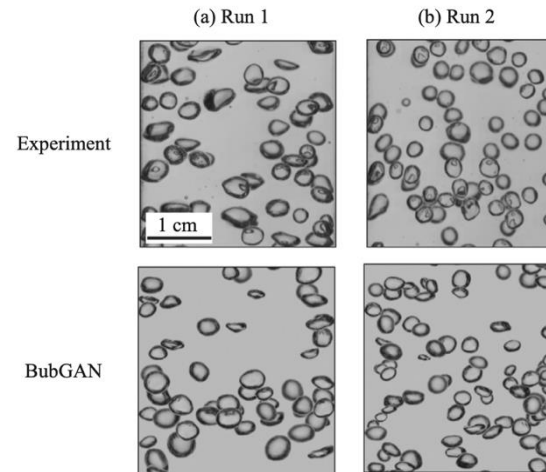
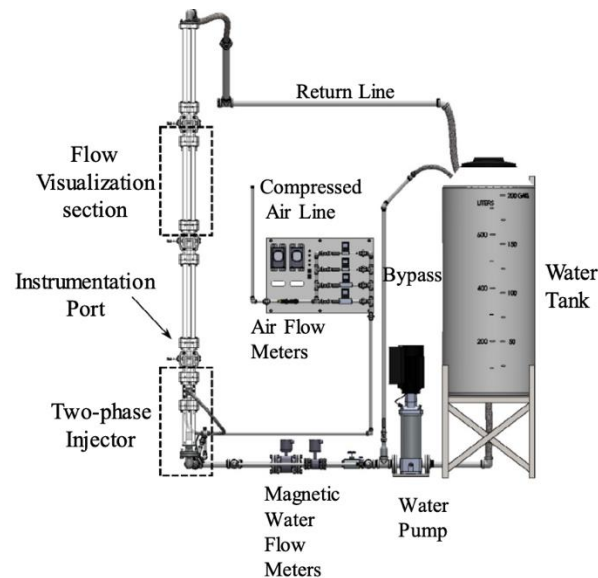
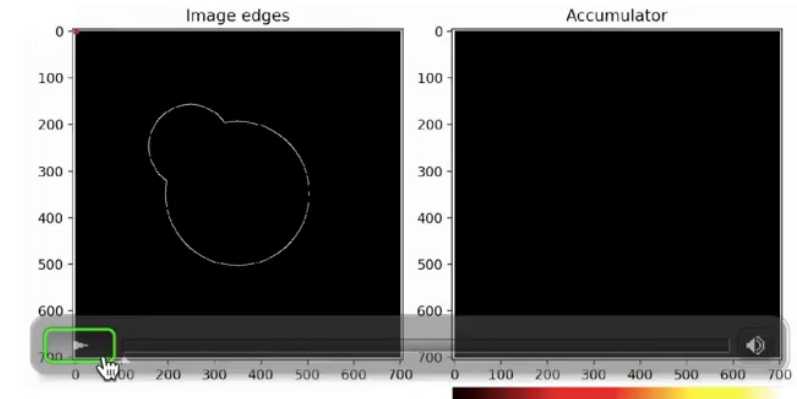


Principle

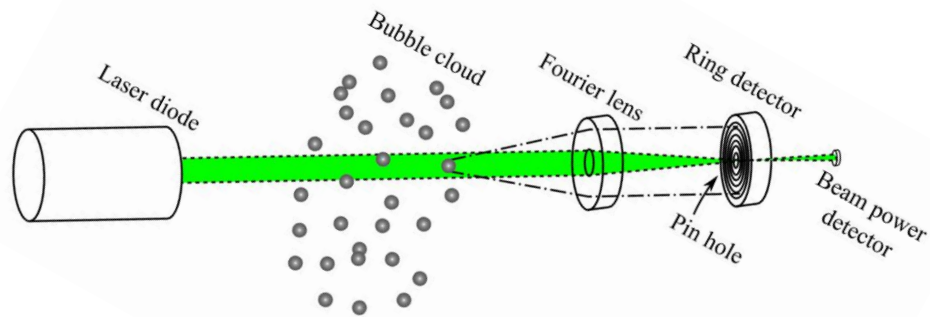
- Bubble illuminated by a diffused light source
- Images recorded by a camera (resolution is important)
- Processing of these backlighting images via a computer algorithm to detect circles/ellipses (fitting procedure).

Image processing challenges

- Circle/Ellipse/Gen. Hough Transform → high storage and computational cost
- High bubble number concentration → bubble overlap
- Breakpoint method for bubble clusters
- Topology analysis (Watershed transform, bubble skeleton, and adaptive threshold)
- Deep learning approaches (BubGAN)
 - Bubbly flow image synthesis



Laser Diffraction systems

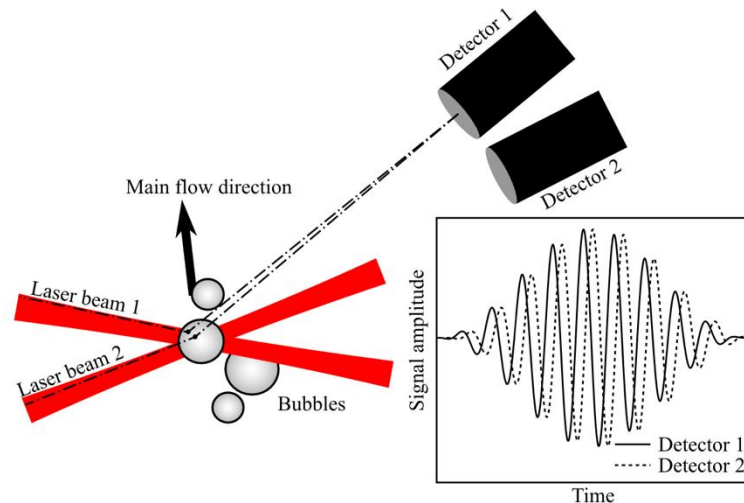


Principle

- Bubbles illuminated by a collimated laser.
- A Fraunhofer diffraction pattern is created, resulting in the original laser beam surrounded by concentric rings in the far-field light intensity.
- Since the radius of the rings is linked to particle diameter, a diameter distribution (averaged along the beam's line of sight) can be determined from the intensity at various radial distances.
- It is a line-of-sight technique.
- It can measure very small bubbles but the fringe intensity can be low.

Laser/Phase Doppler Anemometry

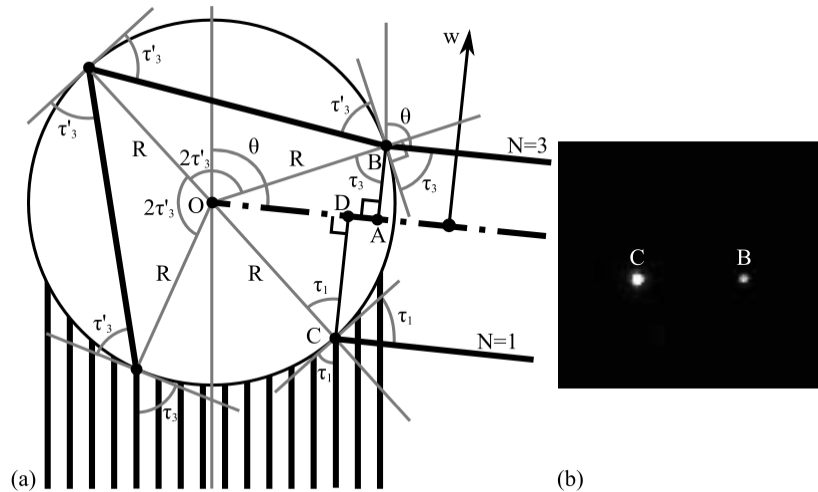
Principle



- In a PDA, a laser Doppler anemometer (LDA) creates a probe volume where two laser beams intersect, forming interference fringes.
- When particles pass through this area, they scatter light.
- Detectors placed at different angles capture the scattered light.
 - **Particle Size Measurement** from the phase shift. By measuring this shift, the PDA can determine the particle's diameter.
 - **Velocity Measurement** from the Doppler shift.

Interaction of a laser with a spherical bubble

Principle

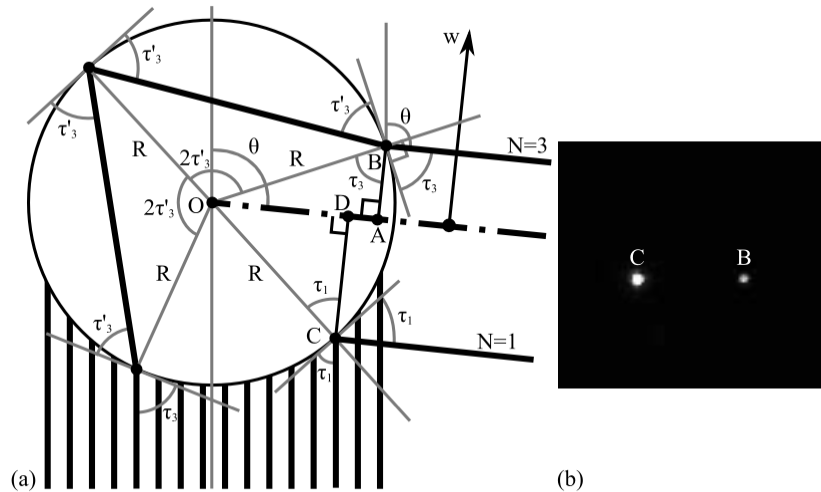


- A laser beam thinner than bubble diameter
- When light rays hit the bubble's surface → reflected or refracted.
 - **Ray 1:** Reflected directly by the bubble (N=1 interaction).
 - **Ray 2:** Undergoes three interactions within the bubble (N=3).
- Both rays exit the bubble at an angle (θ), known as the **observation or scattering angle**
- Since all incoming rays are parallel, they exit at various angles.
- If a camera is positioned far from the bubble at the angle θ relative to the laser, only certain rays (those shown) will reach the camera.
- This creates **high-intensity glare points** at points B and C, where these rays meet the camera view.

The distance between these two high-intensity glare points is proportional to the bubble diameter

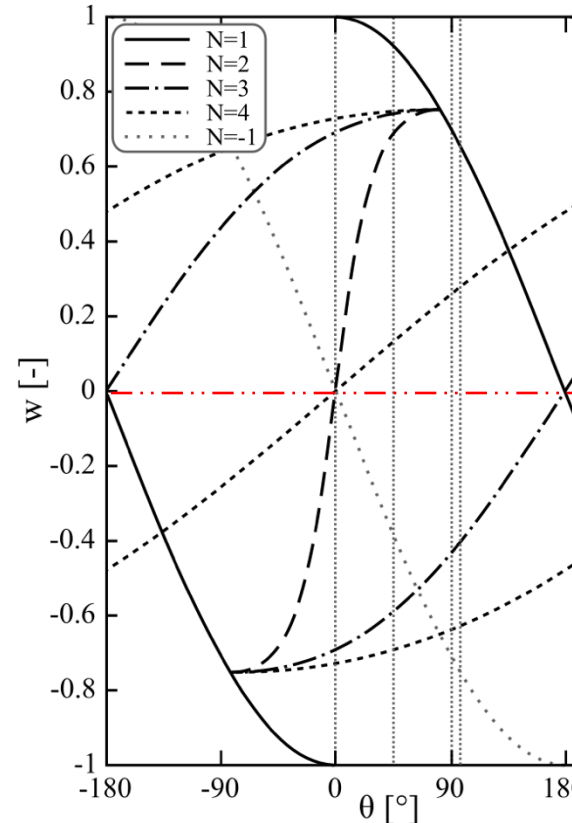
$$D_b = \alpha \delta$$

Observation angle for air bubble in water

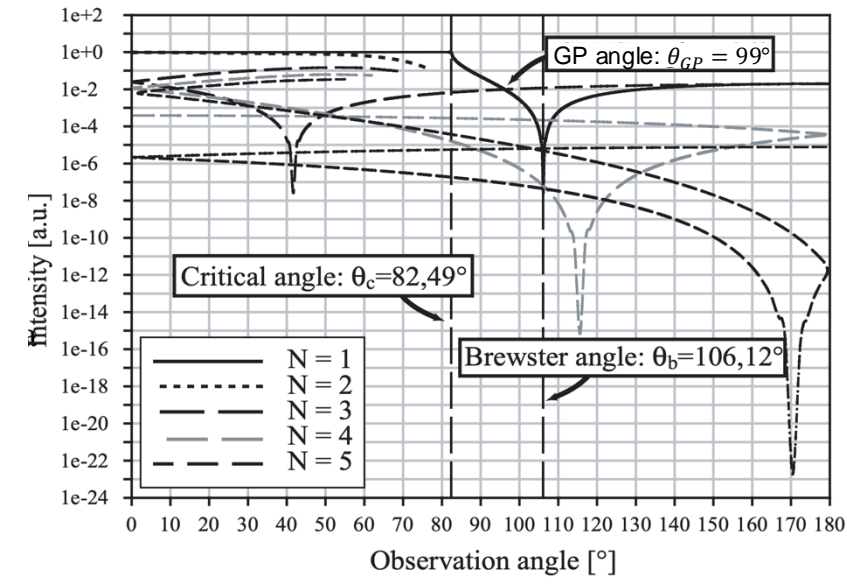


w = distance of the glare point from the middle centerline

$$n_{H_2O} = 1.33, n_{air} = 1$$

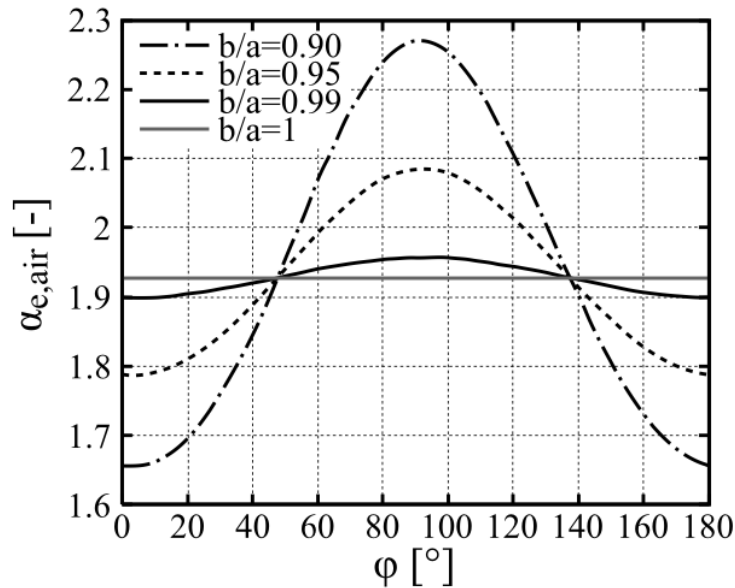
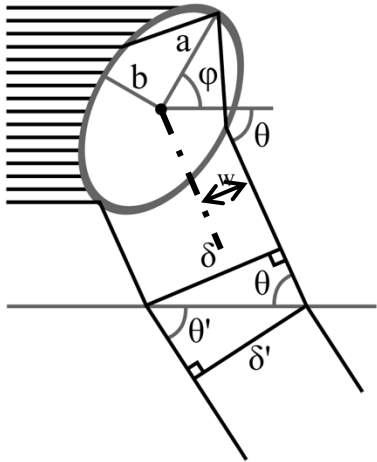


Glare points intensity for parallel polarised laser light



Glare points coming from $N=1$ or $N=3$ have similar intensity at $\theta \cong 99^\circ$

Effect of sphericity, container walls and depth of field

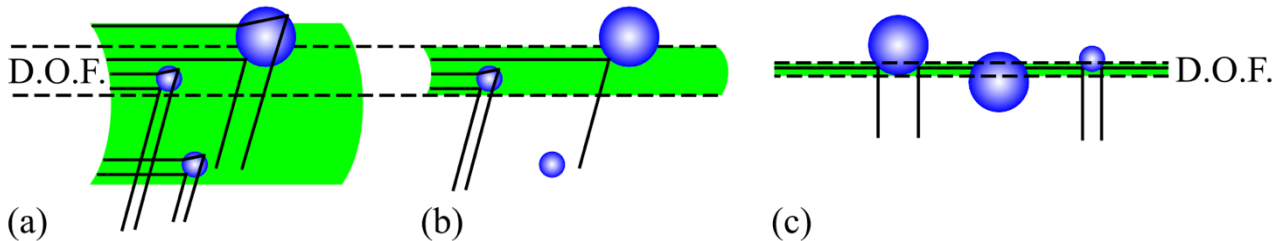


$$\delta' = \frac{\sin \theta'}{\sin \theta} \delta$$

$$\alpha_{1,3} = \frac{2}{\cos\left(\frac{\theta}{2}\right) + \cos \tau_3} \frac{\sin \theta}{\sin \theta'}$$

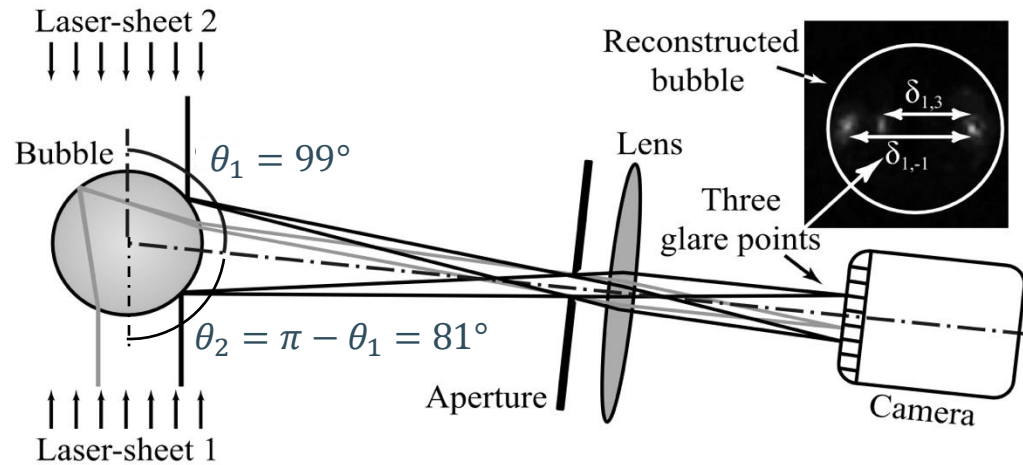
$$D_b = \alpha_{1,3} \delta_{1,3}$$

- Non sphericity plays an important role
- Sphericity cannot be measured, but the presence of non-spherical bubbles can be detected



- This is a 2D approach! The light ray is not allowed to leave the incident plane.
- Hence, the non-sphericity can only be studied when two principal axes lie within this plane.

Extended Glare Point Velocimetry and Sizing



Principle

- Illumination of the bubble on two opposite sides
- With respect to this second illumination, the scattering angle is $\theta_2 = \pi - \theta_1 = 81^\circ$



- Only a third Glare Point appears (N=-1)
- The fourth Glare Point (N=-3) intensity is too weak

$\delta_{1,-1}$ does not depend anymore on the refractive index of the liquid

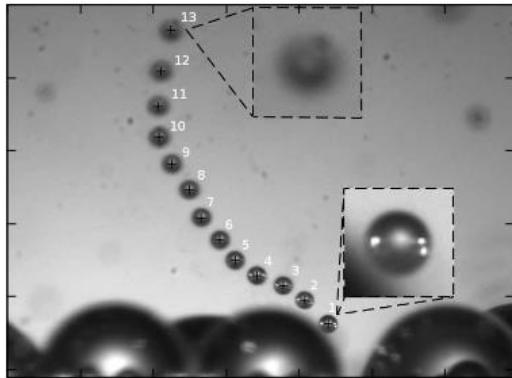
$$\alpha_{1,-1} = \frac{2}{|\sin(\frac{\theta}{2})| + |\cos(\frac{\theta}{2})|} \frac{\sin \theta}{\sin \theta'}$$

Sphericity condition $D_{1,3} = D_{1,-1}$



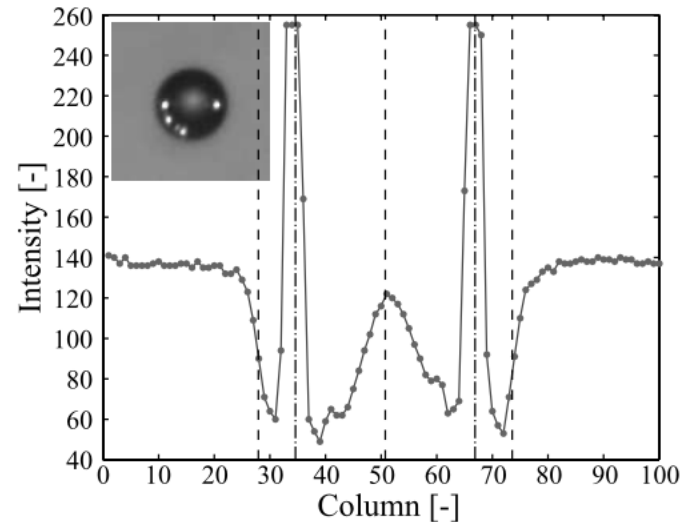
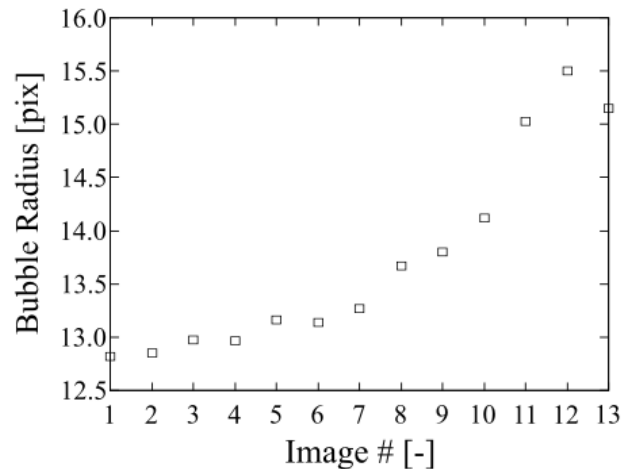
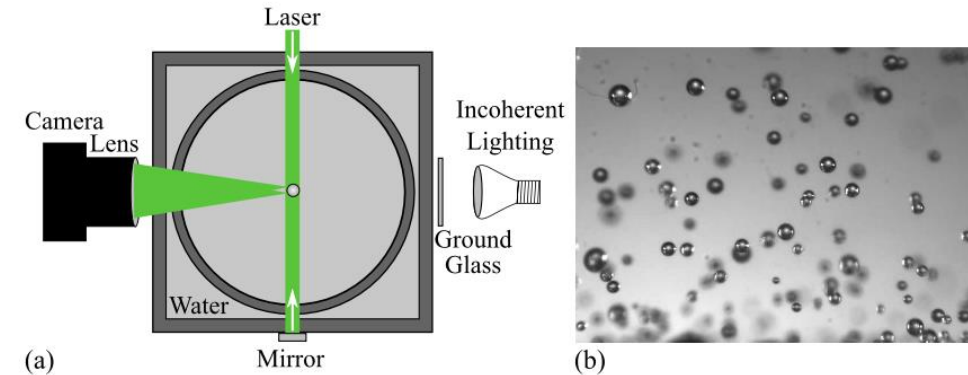
$$\frac{\delta_{1,3}}{\delta_{1,-1}} = \frac{\alpha_{1,-1}}{\alpha_{1,3}}$$

GPVS combined with Backlighting



Principle

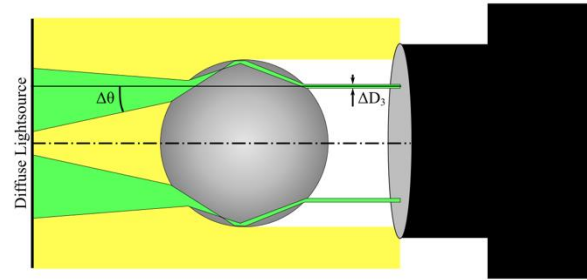
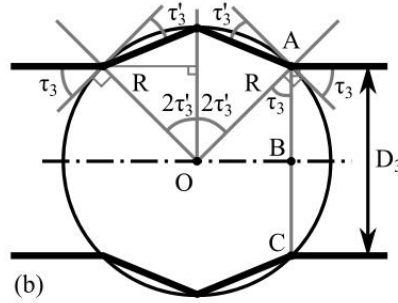
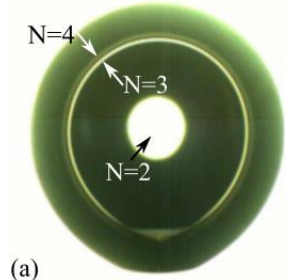
- Illuminate bubbles with laser and diffused light
- Only the bubbles with glare points should be sized as they are well-focused
- Bubbles without glare points can be located closer to or further away from the lens, inevitably leading to sizing errors.



Procedure

- Circle detection (Circle Hough transform).
- Verify the presence of the two Glare Points

Glare Circles

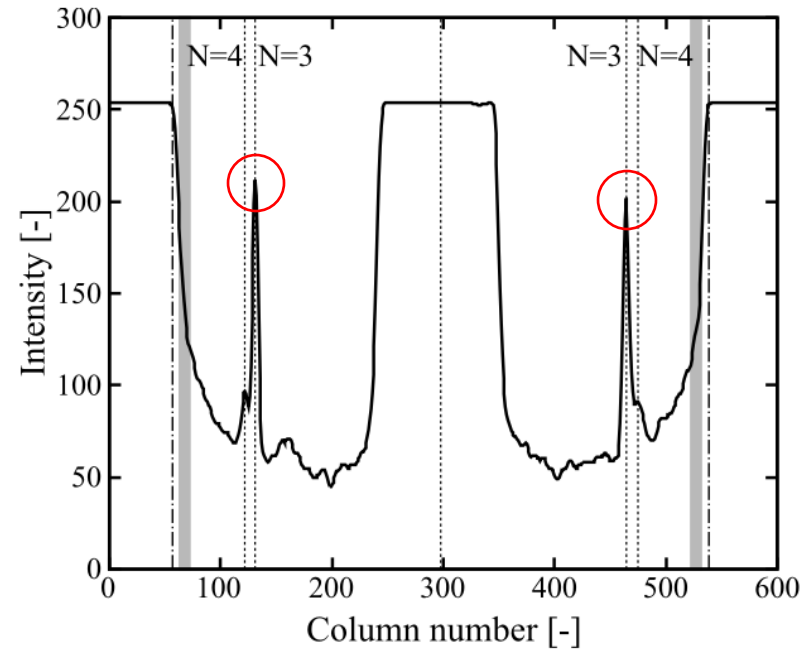


- Principle**
- Line-in-sight observation of bubbles illuminate by diffused light
 - Glare points become circles
 - Glare circle diameter proportional to bubble diameter
 - The glare circle diameter can be estimated with better precision than using Backlight
 - Ratio between Glare and Backlight diameter proportional to refractive index

$$D_3 = \frac{1 + \sqrt{1 + 8n_{liq}^2}}{4n_{liq}^2} D_b$$

Intensity along the diameter of a bubble illuminated by laser and diffused light

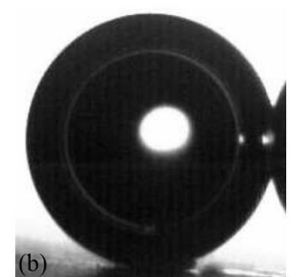
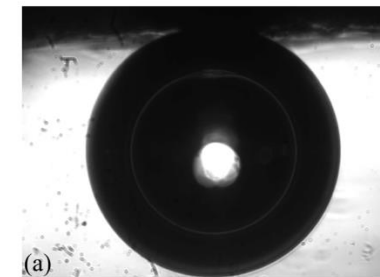
- Backlight gradient ≈ 30 pix
- Glare circle peaks ≈ 8 pix



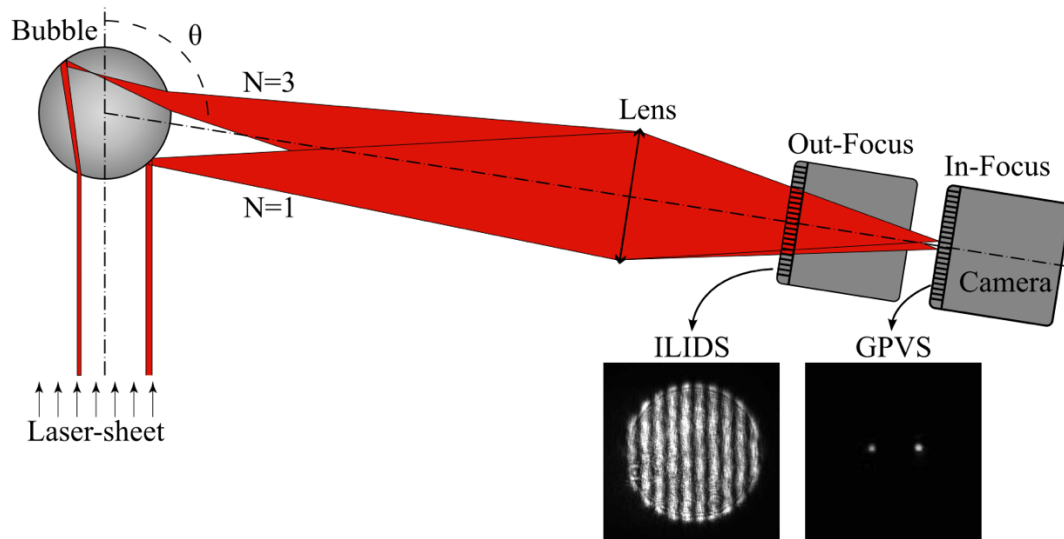
$$\eta = D_3 / D_b \Rightarrow n_{liq} = \sqrt{\frac{1 + \eta}{2\eta^2}}$$

Air/ Silicone oil

Air/ Water



ILIDS

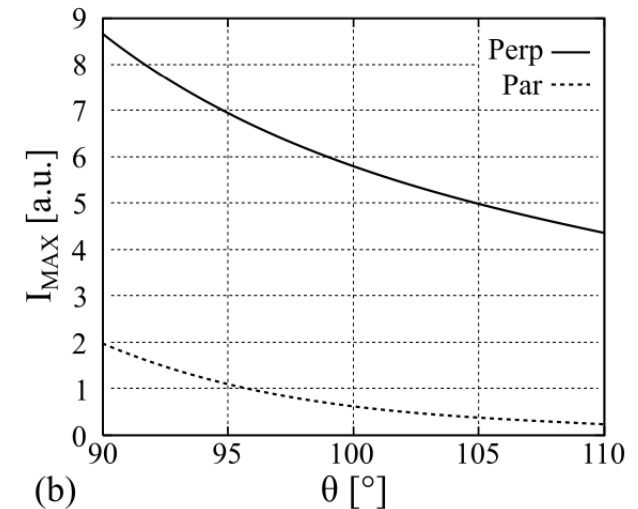
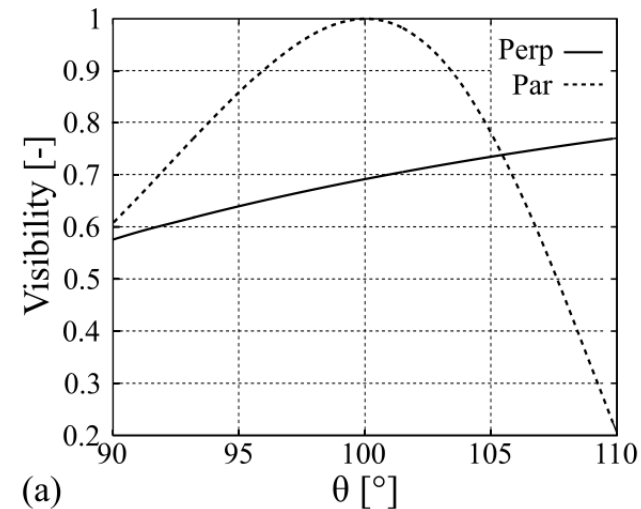


Choice of observation angle based on fringe visibility and Intensity and light polarization

$$Visibility = \frac{I_{max} - I_{min}}{I_{max} + I_{min}} = \frac{2\sqrt{I_1 I_3}}{I_1 + I_3}$$

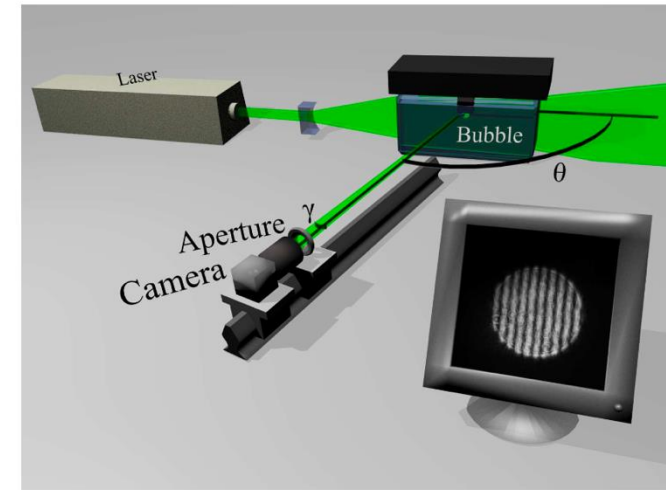
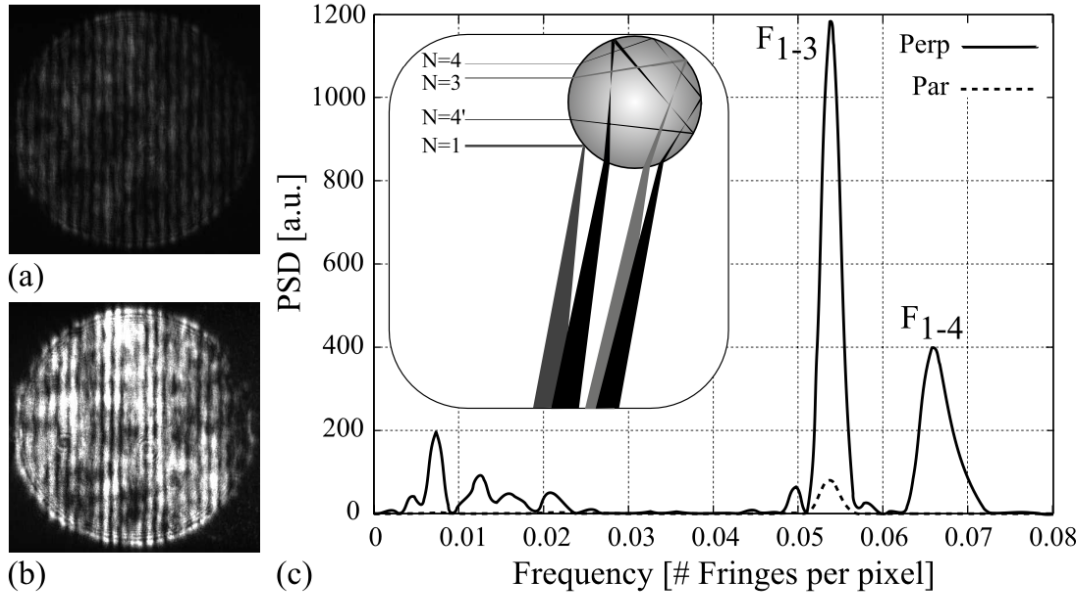
Principle

- Keep geometrical parameters of Glare Points
- Move the optical system out of focus
- Glare points act as coherent point sources → interference
- The diameter of the bubble proportional to the fringe frequency



ILIDS

Fringe analysis and bubble diameter



How to calculate $C_{pix/rad}$?

Methods	Expression
Semi-Experimental Calibration	$C_{pix/rad} = \frac{\Phi_{pix}}{\gamma}$
Theoretical Calibration	$C_{pix/rad} = \frac{gx_o}{fS_{pix}} = \frac{g}{MS_{pix}}$
Camera Focused at Infinity	$C_{pix/rad} = \frac{f}{S_{pix}}$
Two-Step Calibration	$C_{pix/rad} = \frac{fh}{x_{o,if}S_{pix}} = \frac{M_{if}h}{S_{pix}}$

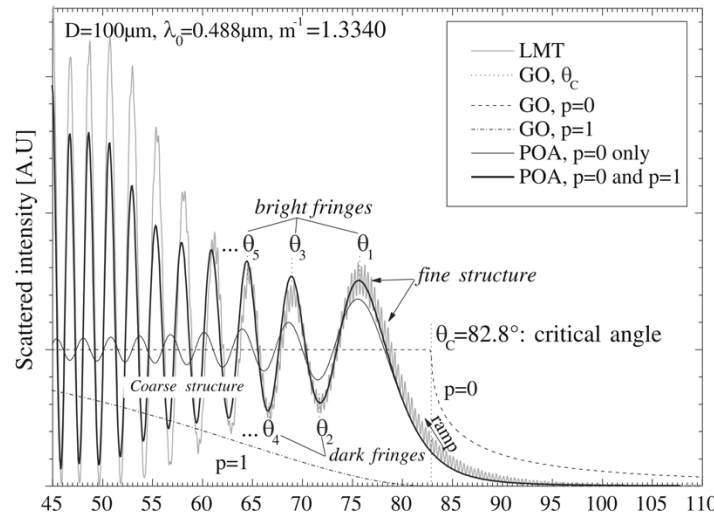
$$D = \lambda \alpha_{1-3} F_{1-3} C_{pix/rad} = \lambda \alpha_{1-4} F_{1-4} C_{pix/rad}$$

$$\text{If spherical bubble } F_{ratio} = \frac{F_{1-3}}{F_{1-4}} = \alpha_{ratio} = \frac{\alpha_{1-4}}{\alpha_{1-3}}$$

Critical Angle Refractometry and Sizing (CARS)

Principle

- The light scattered by a bubble close to the critical angle possesses the diameter signature.
- Fringes are generated in the region close to the critical angle
- A data inversion algorithm is needed to retrieve from the Scattering pattern the bubbles size.



$$p = N - 1$$

$I(\theta, D, m, \lambda_0)$ Intensity of the light scattered by a bubble using Lorentz-Mie theory (LMT)

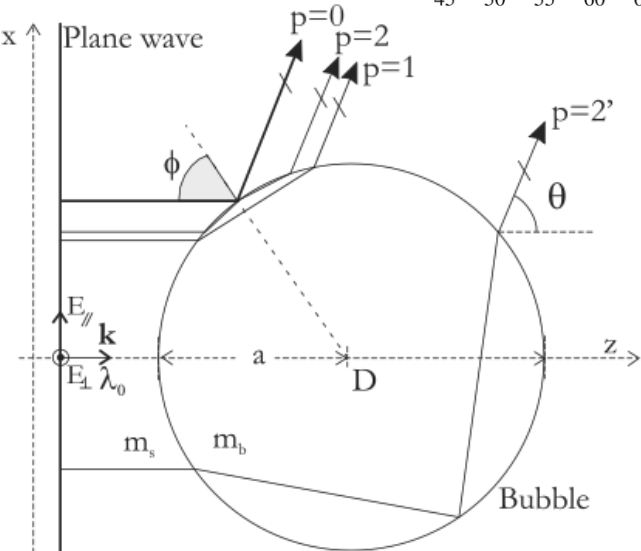
$$I_t(\theta, m, \lambda_0) = N \int_{D_{\min}}^{D_{\max}} I(\theta, D, m, \lambda_0) f(D) dD = \sum_{j=1}^M S_{i,j} F_j$$

$$\Rightarrow \mathbf{I}_t = \mathbf{S} \cdot \mathbf{F}$$

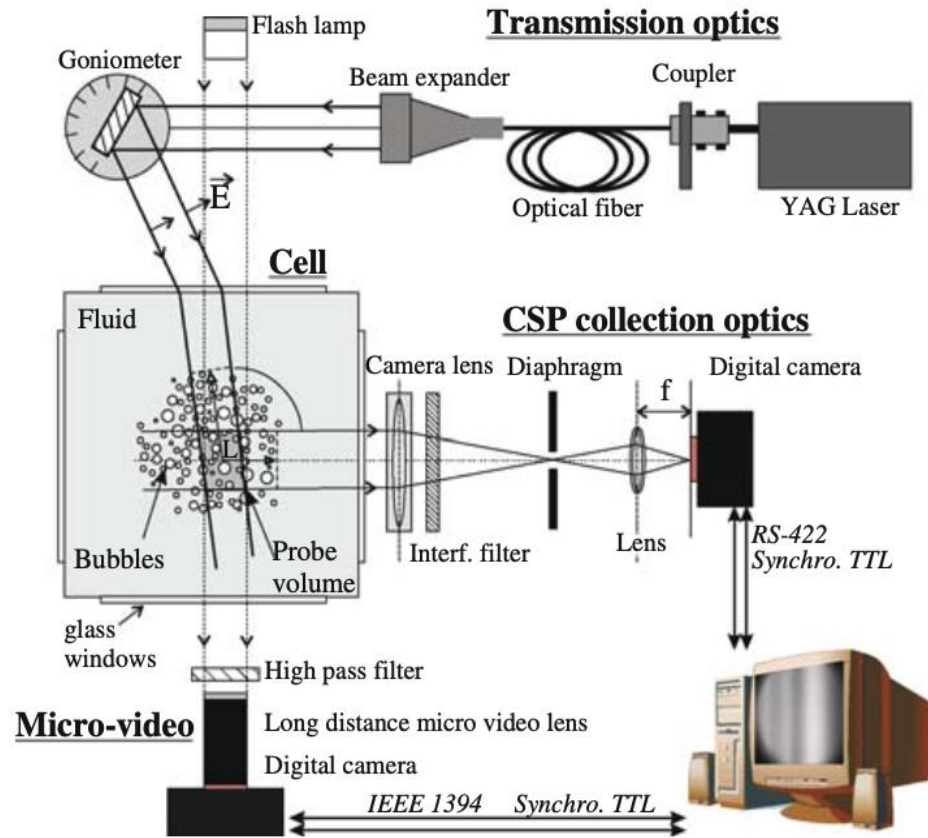
$$\Downarrow$$

$$\leftarrow \mathbf{F} = (\mathbf{S}^T \mathbf{S})^{-1} \mathbf{S}^T \mathbf{I}_t$$

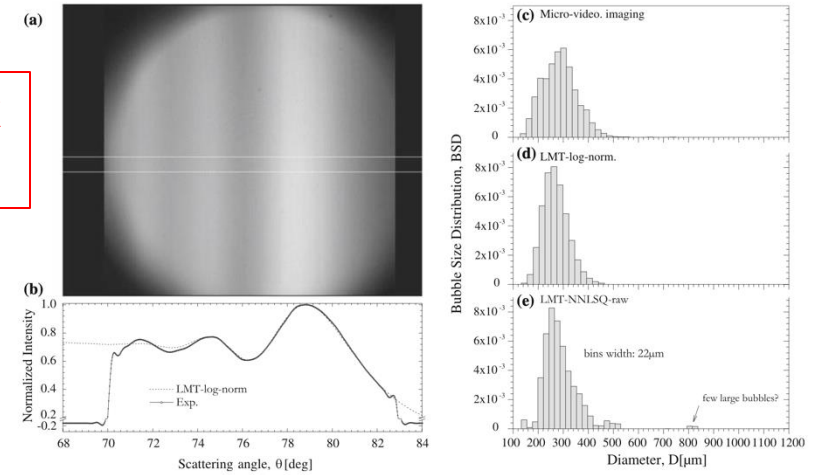
Solution of an ill-posed problem using regularization techniques (Lawson and Hanson)



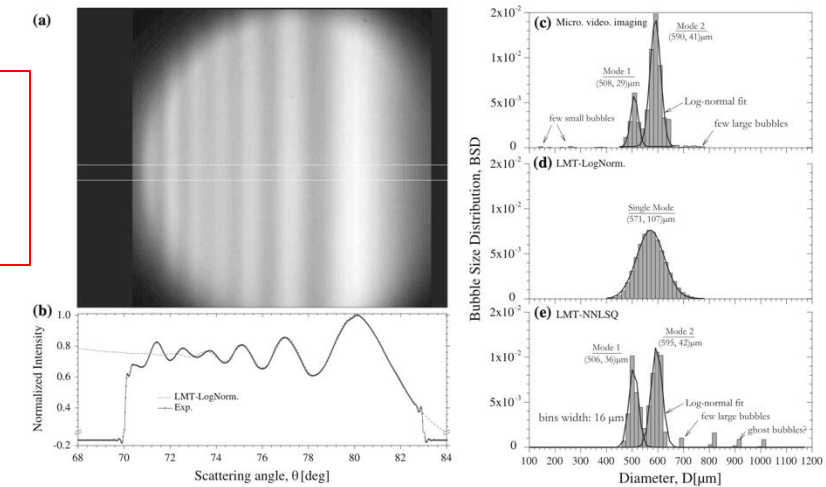
Critical Angle Refractometry and Sizing (CARS)



Single peak distribution



Double peak distribution



Conclusions

- Techniques adapted to void fraction measurements often need preliminary calibration but allow measurements in opaque fluids and may give 2D maps.
- Optical techniques
 - Available on the market (Laser diffraction, PDA, Backlighting).
 - To be developed in laboratory, especially in terms of the data inversion algorithm.
 - Can deliver accurate measurement of bubble size and sometimes refractive index (Temperature!).
 - Often based on light scattering → limited by multiple scattering and therefore bubble concentration.

References

- <http://dx.doi.org/10.3390/fluids5040216>
- <https://doi.org/10.3390/s22093511>
- <http://dx.doi.org/10.1016/j.ces.2014.02.024>
- <http://dx.doi.org/10.1016/j.ijmultiphaseflow.2021.103811>
- <http://dx.doi.org/10.1109/JSEN.2020.3015132>
- <https://doi.org/10.1038/s41598-021-88334-0>
- <https://doi.org/10.1016/j.cryogenics.2018.07.004>
- <https://doi.org/10.1016/j.ijmultiphaseflow.2016.04.011>
- <https://doi.org/10.1016/j.ces.2019.04.004>
- <https://doi.org/10.1007/s00348-009-0649-y>
- <https://doi.org/10.1007/s00348-005-1004-6>
- <https://doi.org/10.1007/s00348-007-0286-2>
- <https://doi.org/10.1007/s00348-008-0502-8>
- <https://doi.org/10.1364/AO.46.005957>
- <https://doi.org/10.1007/s00348-009-0668-8>

Thank you for your attention